J. Geogr. Sci. 2018, 28(10): 1415-1426
DOI: https://doi.org/10.1007/s11442-018-1553-2

The influence of rainfall and land use patterns on soil erosion in multi-scale watersheds: A case study in the hilly and gully area on the Loess Plateau, China

WANG Jun[1], ZHONG Lina[1,2], ZHAO Wenwu[3], YING Lingxiao[1]

1. Land Consolidation and Rehabilitation Center, Key Laboratory of Land Consolidation and Rehabilitation, Ministry of Land and Resources, Beijing 100035, China;
2. School of Land Science and Technology, China University of Geosciences, Beijing 100083, China;
3. College of Resources Science and Technology, Beijing Normal University, Beijing 100875, China

Abstract: Soil erosion has become a major global environmental problem and is particularly acute on the Loess Plateau (LP), China. It is therefore highly important to control this process in order to improve ecosystems, protect ecological security, and maintain the harmonious relationship between humans and nature. We compared the effects of rainfall and land use (LU) patterns on soil erosion in different LP watersheds in this study in order to augment and improve soil erosion models. As most research on this theme has so far been focused on individual study areas, limited analyses of rainfall and LU patterns on soil erosion within different-scale watersheds has so far been performed, a discrepancy which might influence the simulation accuracies of soil erosion models. We therefore developed rainfall and LU pattern indices in this study using the soil erosion evaluation index as a reference and applied them to predict the extent of this process in different-scale watersheds, an approach which is likely to play a crucial role in enabling the comprehensive management of this phenomenon as well as the optimized design of LU patterns. The areas considered in this study included the Qingjian, Fenchuan, Yanhe, and Dali river watersheds. Results showed that the rainfall erosivity factor (*R*) tended to increase in these areas from 2006 to 2012, while the vegetation cover and management factor (*C*) tended to decrease. Results showed that as watershed area increased, the effect of rainfall pattern on soil erosion gradually decreased while patterns in LU trended in the opposite direction, as the relative proportion of woodland decreased and the different forms of steep slope vegetation cover became more homogenous. As watershed area increased, loose soil and craggy terrain properties led to additional gravitational erosion and enhanced the effects of both soil and topography.

Keywords: soil erosion; rainfall; land use patterns; multi-watershed; Loess Plateau

Received: 2017-04-07 **Accepted:** 2018-01-20
Foundation: National Natural Science Foundation of China, No.41771207, No.41171069
Author: Wang Jun (1970–), Professor, specialized in landscape ecology and land sustainable use.
E-mail: wangjun@ lcrc.org.cn

1 Introduction

Soil is a key basic ecosystem component and therefore an important raw material for human life and production (Cerdà *et al*., 2015; Mabit *et al*., 2015). Soil erosion has, however, become more and more widespread globally in recent years and is especially prevalent on the Loess Plateau (LP), China; this phenomenon is now one of the major ecological environmental issues worldwide that is likely to influence the survival and development of humans (Cerdà *et al*., 2014). It is therefore vitally important to prevent and control soil erosion in order to improve the environment, protect ecological security, and to enable harmonious and sustainable development between humans and nature (Govers, 2014; Prosdocimi, 2015).

Research on the impacts of rainfall and land use (LU) on soil erosion has recently become hot topics. For example, Ochoa *et al*. (2016) analyzed the relationship between a number of causative factors including climate, topography, and land cover (LC) at small-scale watersheds and demonstrated the impacts of these factors on soil erosion. In earlier work, Paroissien *et al*. (2015) established a model to simulate the impacts of LU and climate change on soil erosion at the basin scale, and applied this approach to an analysis of annual mean rate of soil erosion in Mediterranean region. The impacts of LU/LC on soil erosion on the LP of China were discussed by Wei *et al*. (2006) who considered the influence of different rainfall patterns; the results of this study showed that the main rainfall factors influencing soil erosion included concentration as well as high intensity and short duration events. Thus, a series of LU types with the ability to resist runoff erosion were ordered in this study from most to least in the sequence of sea-buckthorn, weed, Chinese pine, alfalfa, and wheat. In addition, Zhuang *et al*. (2012) applied the universal soil loss equation (USLE) model to analyze the impacts of LU and rainfall changes on soil erosion in the Xiaojiang River Watershed, part of the Jinsha River in southwestern China. The results of this study highlighted the fact that high intensity soil erosion was mainly distributed at altitudes between 1,600 m and 2,800 m in the downstream part of the Xiaojiang River Watershed. Noteworthily, the bulk of previous research on this topic has been focused mainly on individual watersheds (Iserloh *et al*., 2013; Shi *et al*., 2013; Arhem and Fredén, 2014; Jomaa *et al*., 2014; Gessesse *et al*., 2015); few comparative analyses that address the impacts of rainfall and LU on soil erosion at multi-scale watersheds have been performed. Thus, exploring soil erosion patterns and their variations with rainfall and LU impacts in different watershed areas is important, not only to the research on soil erosion but also to the comprehensive management of regions susceptible to these processes.

Thus, adopting "scale-pattern-process" theory as the basis for research in this area, and considering LU, topography, soil, rainfall, and other factors, the soil loss (SL) evaluation index was initially proposed via the application of methods for calculating related factors in the context of the Revised Universal Soil Loss Equation (RUSLE) model (Zhao *et al*., 2008). A number of previous studies have suggested, however, that the SL index can only provide an approximation of the main processes of soil loss as a component of erosion evaluation; Fu *et al*. (2006) utilized this index in earlier work at small-scale watersheds, calculating it step-by-step based on relevant landscape ecology theory and the main processes of soil erosion. This led to the proposal of a multi-scale SL index (Fu *et al*., 2006), while Zhao *et al*. (2012) provided an additional method for assessment of the vegetation cover and management (*C*) factor between the SL index and the RUSLE model in their study in the Yanhe River Watershed within the hilly and gully area of the LP. The results showed that compared to the *C* factor, the SL index could more accurately describe the impacts of LU patterns on soil erosion while at the same time providing clear scientific reference data enabling reductions in land losses via pattern adjustments within watersheds.

The SL index was improved in this study and applied to the unique hilly and gully terrain area on the LP in northern Shaanxi Province, China. The aim of this study was to explore the effects of rainfall and LU patterns on soil erosion at different watershed scales.

2 Study area

The hilly and gully area on the LP was selected as the study area for this research because it suffers serious soil erosion. This region has a total area of 17,488 km^2 (108°45′–110°25′E and 36°10′–37°55′N, and includes the Qingjian, Fenchuan, Yanhe, and Dali river watersheds (Figure 1). Numerous grooves have formed on the ground surface because of long-term runoff erosion as this area is widely covered by loess soils, having gentle slopes and ridges dissected into tugged topography. With obvious climatic seasonality, average annual rainfall is 513.8 mm and more than 90% of precipitation occurs in May and September. The annual distribution of surface runoff is also concentrated within the flooding season (July–September; sometimes more than 70% of annual runoff can be resulted from just a few rainstorms.

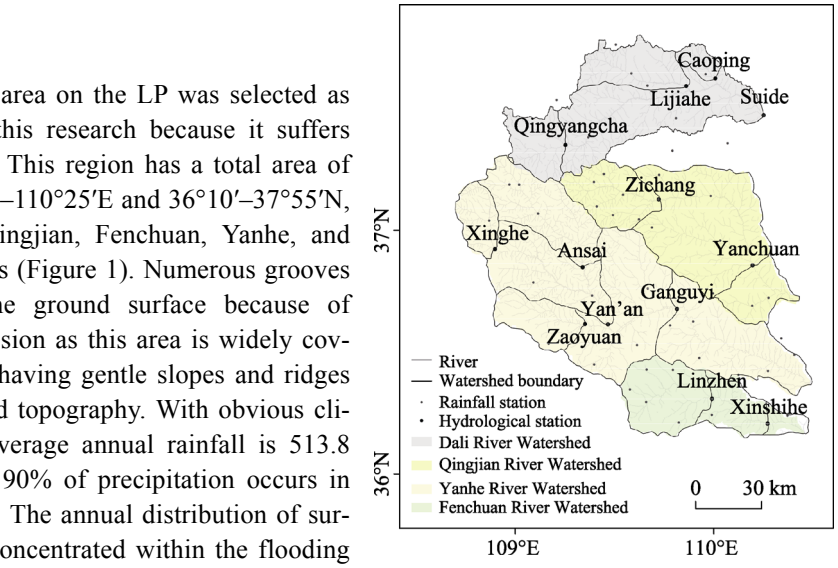

Figure 1 The location of the study area, including watersheds, hydrological and rainfall stations

3 Data collection and methods

3.1 Data

Horizontal and vertical distance as well as slope data were extracted from a digital elevation model (DEM) generated from a 1:5,000,000 scale topographic map using the software ArcGIS 9.3. This enabled the calculation of annual average values for vegetation cover from 2006 to 2012 using Normal Differential Vegetation Index (NDVI) data at a spatial resolution of 500 m extracted from moderate-resolution imaging spectroradiometer (MODIS) (http://www.gscloud.cn/) data. Rainfall, sediment discharge, and other hydrological data collected at 57 rainfall observation stations within the study area were extracted from the *China Hydrological Yearbook: Hydrological Information of the Yellow River Watershed*. The locations of hydrological and rainfall stations are shown in Figure 1.

3.2 Methods

Rainfall and LU patterns refer to the distribution of these parameters in terms of slope and horizontal and vertical distance from river systems. Thus, the closer, more topographically varied, and higher the rainfall and LU pattern unit, the greater the contribution of LU and rainfall pattern to the sediment output of the watershed, and vice versa. We therefore utilized the LU and rainfall pattern indices based on the SL index (Zhao *et al*., 2008), as outlined below.

The SL index was calculated as follows:

$$SL = \frac{f(R,K,T,C)}{f(R,K,T)} \tag{1}$$

where R denotes the rainfall erosivity factor, C denotes the vegetation cover and management factor, K denotes the soil erodibility factor, T denotes the terrain feature factor, and f denotes the function of the SL index at different scales. In this context, SL is a dimensionless factor with values that range between 0 and 1; thus, a larger SL value implies a greater contribution of LU pattern to soil loss, and vice versa.

The rainfall pattern (SL_R) index was calculated based on R and its potential capacity to contribute to soil erosion based on the SL index, as follows:

$$SL_R = \frac{\sum S \times H \times D \times R}{\sum S \times H \times D} \tag{2}$$

where S denotes the slope factor index, while H and D are the horizontal and vertical distance indices of soil loss, respectively.

The LU pattern (SL_C) index was calculated based on the C factor and drawing on the SL index, as follows:

$$SL_C = \frac{\sum S \times H \times D \times C}{\sum S \times H \times D} \tag{3}$$

Calculation of R in this study was based on a simple algorithm for rainfall erosivity within the hilly and gully area on the LP (Zhang, 2003; Zhong, 2015), as follows:

$$R = 0.849 \times \alpha \sum_{j=1}^{k} (X_j)^{\beta} - 29.651 \tag{4}$$

where R denotes the monthly rainfall erosivity [MJ·mm/(ha·h)], while X_j denotes erosive rainfall on day j. Erosive rainfall request rainfall is greater than, or equal to, 12 mm, if it is erosive rainfall equal to rainfall, or is otherwise calculated as zero; thus:

$$\beta = 0.8363 + 18.44 P_{d_{12}}^{-1} + 24.455 P_{y_{12}}^{-1} \tag{5}$$

and

$$\alpha = 21.586 \beta^{-7.1891} \tag{6}$$

where P_{d12} denotes daily average rainfall greater than, or equal to, 12 mm, while P_{y12} refers to the annual average daily rainfall greater than, or equal to, 12 mm.

The relationship between the C factor and crop coverage is complicated. Thus, the first of these two variables was calculated as follows (Cai *et al*., 2000):

$$F_c = (NDVI - NDVI_{\min}) / (NDVI_{\max} - NDVI_{\min}) \tag{7}$$

$$\begin{cases} C = 1 & F_c = 0 \quad (8) \\ C = 0.6508 - 0.3436 \lg F_c & 0 < F_c < 78.3\% \quad (9) \\ C = 0 & F_c \geqslant 78.3\% \quad (10) \end{cases}$$

where F_c refers to the extent of vegetation coverage, while $NDVI_{\min}$ and $NDVI_{\max}$ denote the minimum and maximum values of the NDVI within the study area, respectively.

The soil loss distance index reflects differences in the degree of contribution of various LU types to river sediment as a function of distance from the water system (Zhao *et al*., 2008). These LU type distances can be further divided both horizontally and vertically (Figure 2); thus, d_i denotes the horizontal distance of soil erosion at point i in a small watershed, while h_i denotes the vertical distance at the same point. Applying the Straight Line function of the Spatial Analyst tool in the software ArcGIS v9.3 enabled us to extract the horizontal distance of point i from the river system based on the spatial distribution map. In contrast, extracting a measure for vertical

soil erosion was relatively more complicated, and was achieved in a series of distinct steps. Water vector data was first converted to a raster format and a grid value of 1 was defined prior to application of the raster calculator module in ArcGIS v9.3. The water grid was then multiplied with DEM data to obtain a map comprising elevation values which were then extended outwards so that the water surface covered the entirety of a small watershed (i.e., the surface of a river system). Finally, a vertical distance map of soil loss was obtained by subtracting DEM data from values for water level elevation; horizontal (D) and vertical (H) distance indices were then calculated based on corresponding soil losses.

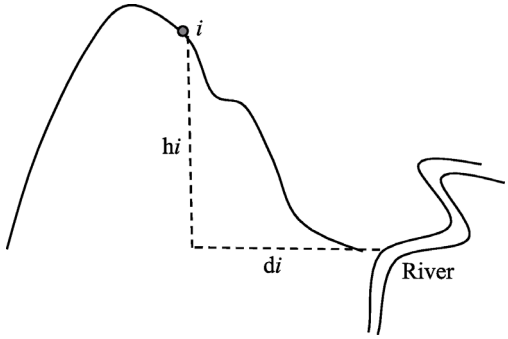

Figure 2 Schematic diagram of horizontal distance (h_i) and vertical distance (d_i) of soil loss (Zhao *et al*., 2008)

Values of D were calculated as follows:

$$D_i = \frac{D_{\max} - d_i}{D_{\max}} \tag{11}$$

where D_i denotes the soil erosion distance index at one point within a watershed, while $D_{\max}$ denotes the maximum value of this index within a watershed, and d_i denotes the soil erosion distance at a given point within a watershed. Soil erosion distance in this context refers to the minimum straight line distance from one point along the sediment transport path to the water system within a watershed.

Values of H were calculated as follows:

$$H_i = \frac{H_{\max} - h_i}{H_{\max}} \tag{12}$$

where H_i denotes the soil erosion vertical distance index at one point within a watershed, while $H_{\max}$ denotes the maximum value of soil erosion vertical distance, and h_i denotes the vertical distance of soil erosion at a given point within a watershed.

Values of S were calculated as follows (Liu *et al*., 1994).

$$S_i' = 21.91\sin\theta - 0.96 \tag{13}$$

and

$$S_i = \frac{\left(S_i' - S_{i\min}'\right)}{\left(S_{i\max}' - S_{i\min}'\right)} \tag{14}$$

where S_i denotes the slope factor index, θ refers to the slope gradient, S_i' refers to the slope factor, and $S_{\min}'$ and $S_{\max}'$ denote the minimum and maximum slope factors, respectively, within the watershed.

4 Results

4.1 Characteristics of factors in SL_R and SL_C

4.1.1 Characteristics of rainfall erosivity factor (R)

Values of R for 57 rainfall observation stations within the hilly and gully study area on the LP for the period from 2006 to 2012 were calculated by using the simple algorithm presented by Zhang *et al*. (2003), and a distribution map was generated (Figure 3). Results showed that R values for

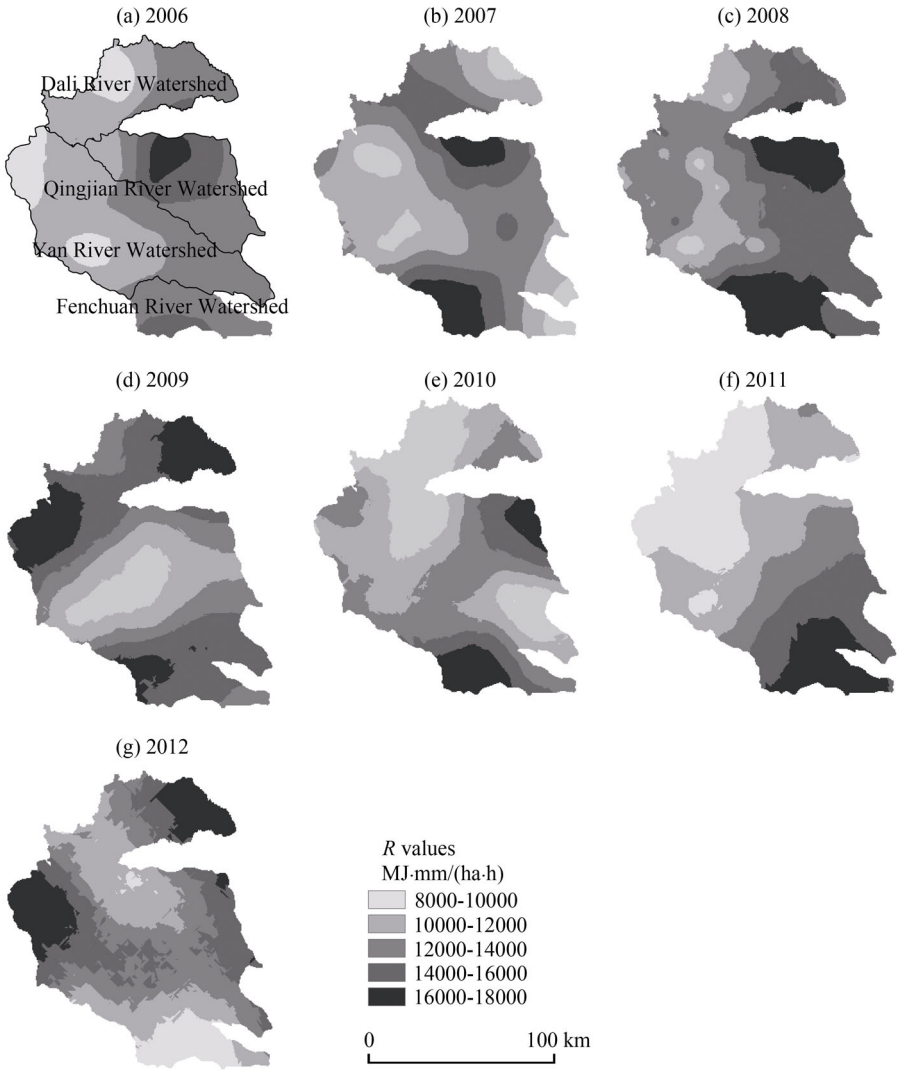

Figure 3 The spatial distribution of *R* factor from 2006 to 2012 within the hilly and gully area on the LP

the Yanhe and Dali river watersheds remained generally low, while the opposite was the case for the watersheds of the Qingjian and Fenchuan rivers. Similarly, *R* values for upstream regions of the Fenchuan and Qingjian river watersheds remained relatively high while those for downstream regions were relatively low over the time period of this study; the opposite pattern was detected in the Yanhe and Dali river watersheds. Two upstream zones with high *R* values were identified within the Qingjian and Fenchuan river watersheds, while low value zones were identified in the upstream area of the Dali River Watershed and in the mid-upstream of the Yanhe River Watershed. The inter-annual variation in *R* within the study area was illustrated in Figure 4; these data showed that *R* tended to increase

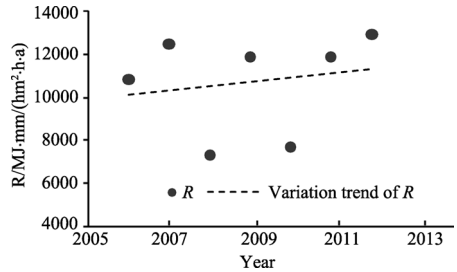

Figure 4 Inter-annual variation in R within the hilly and gully area on the LP from 2006 to 2012

from 2006 to 2012 (P=0.05), although values were relatively low in both 2008 and 2010 because the volume of rainfall was also relatively small in these years.

4.1.2 Characteristics of *C*

The distribution of *C* values was shown in Figure 5. The results suggested that *C* values for the Dali River Watershed in the north of the study area remained relatively high throughout the study period while those of the Fenchuan River Watershed in the south were relatively low. At the same time, *C* values tended to decline along a north-south transect across the study area over the course of this research. The results presented in Figure 6 were generated by calculating annual average *C* values and reveal an overall downward trend from 2006 to 2012 (P=0.05). This LP study area is noteworthy because it has experienced the implementation of a policy to return farmland to forests and grasslands since 1998; the results of this process have been remarkable as vegetation coverage has significantly increased, and ecological environmental quality has significantly improved since 2000. Vegetation coverage in this region has also consistently increased year by year due to the continuous return of farmland to forests and grasslands (Zhong

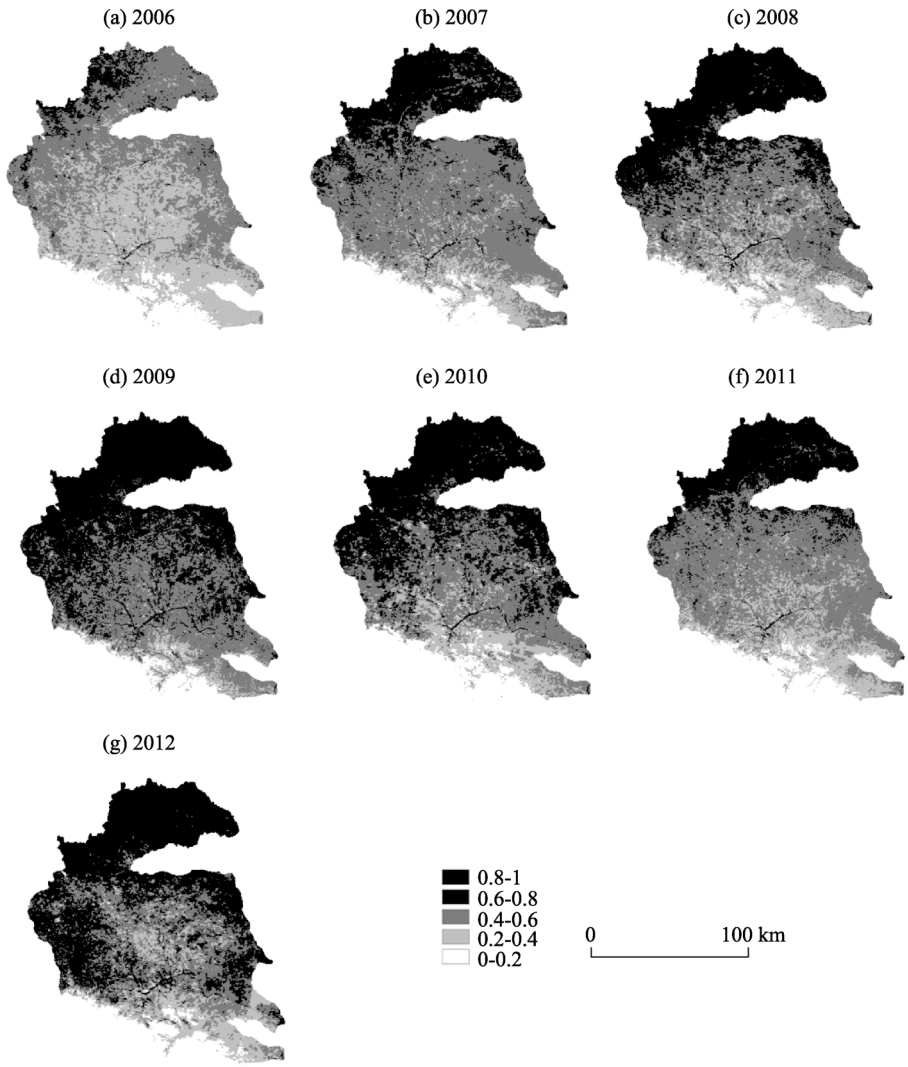

Figure 5 The spatial distribution of *C* within the hilly and gully area on the LP from 2006 to 2012

and Zhao, 2013); a close relationship between the *C* and vegetation coverage was revealed, while Equations (7) to (9) showed that these values decreased from 2006 to 2012.

4.1.3 Other factors

Minimum line distances and the vertical distance between points and the water system were extracted from DEM data alongside slope gradient values to enable the calculation of *D*, *H*, and *S* (Figure 7).

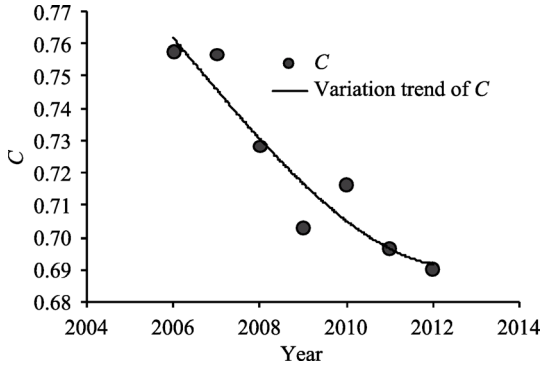

Figure 6 Inter-annual variation in values of the *C* within the hilly and gully area on the LP from 2006 to 2012

Figure 7 The patterns of *D*, *H*, and *S* within the hilly and gully area on the LP

4.2 The impact of rainfall patterns on soil erosion within multi-watersheds

Values of SL_R from 2006 to 2012 for 13 small watersheds were calculated as part of this study. These results enabled evaluation of the impact of rainfall pattern on soil erosion within multi-watersheds via the calculation and analysis of correlation coefficients between SL_R and sediment discharge data for the 13 small watersheds (P=0.05). Figure 8 revealed that the impacts of rainfall pattern on soil erosion gradually decreased as watershed area increased. In other words, the smaller the watershed area, the greater the contribution of rainfall patterns to soil erosion, and vice versa.

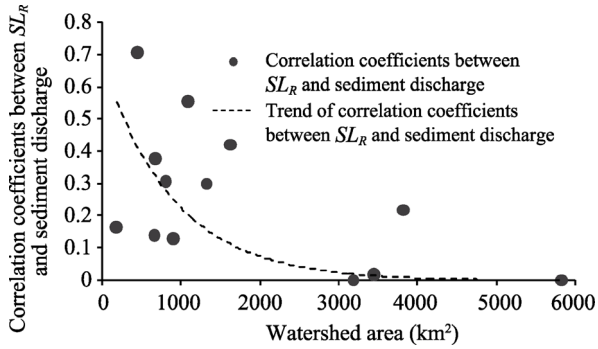

Figure 8 The effect of rainfall pattern on soil erosion in different watersheds in the hilly and gully area on the LP

4.3 The impact of LU patterns on soil erosion in multi-watersheds

Values of SL_C from 2006 to 2012 for 13 small watersheds were calculated as part of this study. These data enabled evaluation of the impact of LU patterns on soil erosion within multi-watersheds via calculation and analysis of correlation coefficients between SL_C and sediment discharge data for the 13 small watersheds (P=0.05). Figure 9 showed that the impact of LU patterns on soil erosion gradually increased in concert with watershed area. In other words, the

smaller a watershed area, the smaller the contribution of LU patterns to soil erosion, and vice versa.

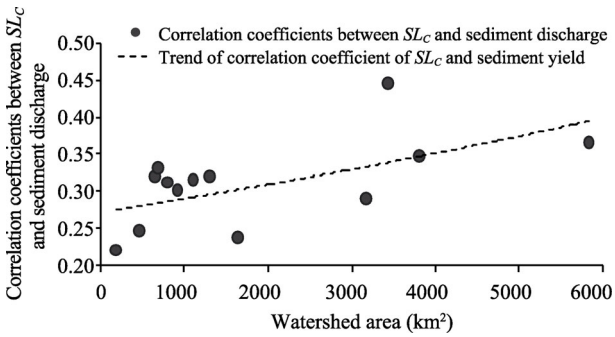

Figure 9 The effect of LU patterns on soil erosion in different watersheds within the hilly and gully area on the LP

4.4 A comparative analysis of the effect of rainfall and LU patterns on soil erosion within different watershed areas

The data presented in Figure 10 was generated by comparing the correlation coefficients between either SL_R or SL_C and sediment discharge (Figure 10). These data show that correlation coefficients between SL_R and sediment discharge were greater than those seen for SL_C in the case of the seven watersheds in Caoping, Xinghe, Qingyangcha, Zaoyuan, Lijiahe, Zichang, and Linzhen, while the opposite was true for the six watersheds within Ansai, Suide, Xinshihe, Yan'an, Yanchun, and Ganguyi. Indeed, watershed area increased from left to right along the horizontal axis (Figure 10); this meant that the effect of rainfall pattern on soil erosion was larger than that of LU pattern when a watershed was relatively smaller, and vice versa at relatively larger sizes.

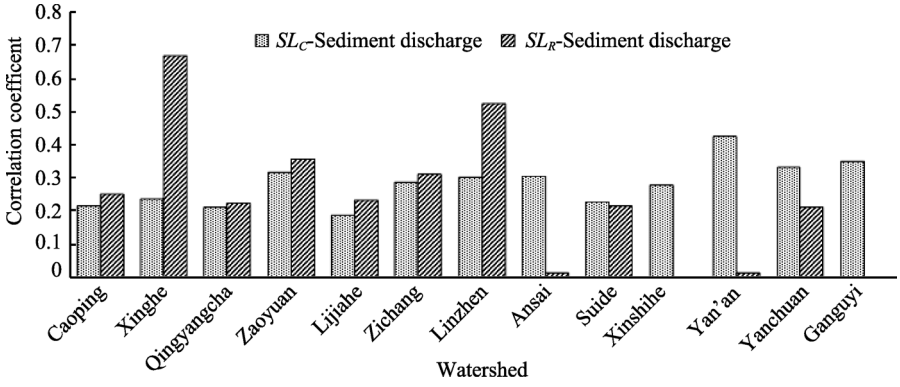

Figure 10 Comparison of the effects of rainfall and LU patterns on soil erosion in 13 watersheds within the hilly and gully area on the LP

4.5 Causal analysis

It is clear that soil erosion is the combined result of rainfall, LU, topography, soil type, and other factors. A great many variables influence this complex process; the results presented in this study showed that the influence of rainfall on soil erosion was greater than that of LU pattern when the watershed area was smaller. While, the influence of LU pattern on soil erosion was more dominant as watershed area increased; it is clear, for example, that different patterns of LU influence the emergence of runoff by changing underlying surface features. In order to ensure ongoing survival and development, humans have constantly modified their land surface environments, and such changes in LU patterns are one of the important ways that anthropogenic activities adapt to the environment (Wu *et al*., 2014). Thus, the influence of LU patterns on soil erosion actually reflects human activities; the return of farmland to forests and grasslands has been the dominant human activity within this study area since 1998 and has led to significant increases in

vegetation coverage, largely changing local LU patterns.

Ding *et al*. (2015) have noted that vegetation cover types tend to be monospecific as watershed area increases within the hilly and gully area on the LP in northern Shaanxi Province when the proportion of grassland increases in concert with a reduction in forested land and farmland. And compared to grassland and cultivated land, forests tend to have much better soil-water storage and conservation capacities. This change of vegetation is the main reason for the increase of the effects of LU pattern on soil erosion as watershed area increases. This also indicates that the effect of human activities on soil erosion increases when watershed areas are relatively larger.

It has also been noted in previous work that soil erosion within a watershed is mainly the result of splash, sheet, and rill erosive effects (Liu, *et al*., 2004). Specifically, rills cut down into the soil and subsoil and gradually develop into shallow gullies; runoff therefore collects in these gullies, cuts down into their base, and extends channels and heads of gullies stretch upwards to form broken dissected surface owing to the gully erosion. The amount of sediment yield caused by this process nevertheless remains small and stable when splash erosion dominates, while the direct impacts of rainfall are relatively more significant. It is the case, therefore, that the sediment yield caused by erosion increases when these processes are dominated by shallow gully mechanisms; under such situations, rainfall, soil, and LU are all significant factors influencing erosion, while sediment is mainly derived from the collapse of cut channel walls and the development of trenches. The sediment yield that results from erosion increases significantly when linear processes, including gravity erosion, become dominant (Jia *et al*., 2005); consequently, soft soil and the crisscrossed ravine networks that form increase the probability of gravitational erosion and enhance the impacts of both soil and topography.

5 Discussion

In their earlier work, Hu *et al*. (2014) proposed that the value of R factor had decreased from the south to the northwest between 1971 and 2012 in Shaanxi Province. The results of this study lend themselves to a similar conclusion; calculated *R* values for the Yanhe and Dali river watersheds in the northern part of the study area were relatively smaller while values for the Qingjian and Fenchuan river watersheds in the south were relatively higher. Numerous scholars have examined the spatiotemporal characteristics of vegetation coverage on the LP and have suggested that an increase occurred from 2006 to 2012 (Liu *et al*., 2011; Wei *et al*., 2017). And it was also shown that vegetation coverage is high in the southeast and low in the northwest of the plateau. Because the negative correlation in vegetation coverage and *C* factor, the *C* factor has tended to decline from 2006 to 2012 and was low in the south and high in the north. The conclusion of Wei *et al*. (2006) that there is great difference between runoff and soil erosion given different rainfall and LU patterns is supported by this study.

The SL index includes soil erosion spatial distribution information and also reflects loss processes at different scales. However, the relevant factors that comprise this index remain too numerous and complicated to calculate. Horizontal and vertical distance from the river system as well as slope factor following deletion of the superfluous factor in LU pattern were used in this study to generate an alternative LU pattern index that could reflect the effects of this variable on soil erosion. A further rainfall pattern index was also proposed in this study that was based on the LU pattern index. Data for these revised indices are easy to collect, and they are relatively simple to calculate; use of these approaches can therefore more accurately reflect the impacts of rainfall and LU patterns on soil erosion.

Soil erosion is the combined result of rainfall, LU, soil type, topography, tillage, management, and other factors. The emphasis in this paper has been on analyzing the impacts of rainfall and LU patterns on soil erosion without taking their spatial correlations into account. Thus, examining the spatial distribution patterns of rainfall, LU, soil type, topography, tillage, management methods, and other factors, as well as considering the relationships and correlations between them and their influence on soil erosion as watershed areas change should be explored in future work.

6 Conclusions

Building based on the SL index, and combining horizontal and vertical distance from the river system in tandem with slope factor, pattern indices for rainfall and LU are developed in this paper and their impacts on soil erosion in multi-watersheds on the LP in northern Shaanxi Province are discussed. A number of clear conclusions are presented as a result of this research.

(1) Values for *R* from 2006 to 2012 within the study area tended to generally increase, while the opposite trend was seen in *C* values.

(2) As watershed area increased, the impact of rainfall pattern on soil erosion within the study area tended to gradually decrease, while the impact of LU pattern gradually increased. When the watershed area was small, the impact of rainfall pattern on soil erosion tended to be larger than that of LU pattern. The opposite was suggested when watershed area was large.

(3) As watershed area increased, the proportion of forested land tended to decrease and vegetation cover types tended to be monospecific. This phenomenon was the main explanation for an overall increase of the effect of LU patterns on soil erosion within watersheds. At the same time, the effect of rainfall on soil erosion tended to be relatively large when a watershed was relatively smaller, while the impacts of soil and topography on erosion increased in concert with watershed area.

References

Arhem K, Fredén F, 2014. Land cover change and its influence on soil erosion in the Mara region, Tanzania: Using satellite remote sensing and the Revised Universal Soil Loss Equation (RUSLE) to map land degradation between 1986 and 2013. Lund: Lund University.

Cai Chongfa, Ding Shuwen, Shi Zhihua *et al*., 2000. Study of applying USLE and geographical information system IDRISI to predict soil erosion in small watershed. *Journal of Soil and Water Conservation*, 14(2): 19–24. (in Chinese)

Cerdà A, Jordán A, Zavala L *et al*., 2014. The contribution of mulches to control high soil erosion rates in vineyards in eastern Spain. *EGU General Assembly Conference Abstracts*, 16: 16127.

Cerdà A, Pelayo Ó G, Pereira P *et al*., 2015. The wild geographer avatar shows how to measure soil erosion rates by means of a rainfall simulator. *EGU General Assembly Conference Abstracts*, 17: 15878.

Ding Jingyi, Zhao Wenwu, Wang Jun *et al*., 2015. Scale effect of the impact on runoff of variations in precipitation/vegetation: Taking northern Shaanxi loess hilly-gully region as an example. *Progress in Geography*, 34(8): 1039–1051. (in Chinese)

Fu Bojie, Zhao Wenwu, Chen Liding *et al*., 2006. Multi-scale soil loss evaluation index. *Chinese Science Bulletin*, 51(16): 1936–1943. (in Chinese)

Gessesse B, Bewket W, Bräuning A, 2015. Model-based characterization and monitoring of runoff and soil erosion in response to land use/land cover changes in the Modjo watershed, Ethiopia. *Land Degradation & Development*, 26(7): 711–724.

Govers G, Van Oost K, Wang Z, 2014. Scratching the critical zone: The global footprint of agricultural soil erosion. *Procedia Earth and Planetary Science*, 10: 313–318.

Hu Lin, Su Jing, Sang Yongzhi *et al*., 2014. Spatial and temporal characteristics of rainfall erosivity in Shaanxi Province. *Arid Land Geography*, 37(6): 1101–1107. (in Chinese)

Iserloh T, Fister W, Marzen M *et al*., 2013. The role of wind-driven rain for soil erosion–an experimental approach. *Zeitschrift für Geomorphologie, Supplementary Issues*, 57(1): 193–201.

Jia Yuanyuan, Zheng Fenli, Yang Qinke, 2005. Distributed water erosion prediction model for small watershed in loess plateau. *Journal of Hydraulic Engineering*, 36(3): 328–332. (in Chinese)

Jomaa S, Barry D A, Brovelli A *et al*., 2012. Rain splash soil erosion estimation in the presence of rock fragments. *Catena*, 92: 38–48.

Leys A, Govers G, Gillijns K *et al*., 2010. Scale effects on runoff and erosion losses from arable land under conservation and conventional tillage: The role of residue cover. *Journal of Hydrology*, 390(3): 143–154.

Liu B Y, Nearing M A, Risse L M, 1994. Slope gradient effects on soil loss for steep slopes. *Transactions of the ASAE*, 37(6): 1835–1840.

Liu Qingquan, Li Jiachun, Chen Li *et al*., 2011. Dynamics of overlan flow and soil erosion (II): Soil erosion. *Advances in Mechanics*, 34(4): 493–506. (in Chinese)

Liu Zhihong, Guo Weiling, Yang Qinke *et al*., 2011. Vegetation cove rchanges and their relationship with rainfall in different physiognomy type areas of Loess Plateau. *Science of Soil and Water Conservation*, 9(1): 16–23. (in Chinese)

Mabit L, Zapata F, Dercon G *et al*., 2014. Assessment of soil erosion and sedimentation: The role of fallout radionuclides. *Iaea Tecdoc Series*, 3: 181–201.

Ochoa P A, Fries A, Mejía D *et al*., 2016. Effects of climate, land cover and topography on soil erosion risk in a semiarid basin of the Andes. *Catena*, 140: 31–42.

Paroissien J B, Darboux F, Couturier A *et al*., 2015. A method for modeling the effects of climate and land use changes on erosion and sustainability of soil in a Mediterranean watershed (Languedoc, France). *Journal of Environmental Management*, 150(1): 57–68.

Peter K D, Doleire-Oltmanns S, Ries J B *et al*., 2014. Soil erosion in gully catchments affected by land-levelling measures in the Souss Basin, Morocco, analysed by rainfall simulation and UAV remote sensing data. *Catena*, 113: 24–40.

Prosdocimi M, Cerdà A, Tarolli P, 2015. Soil water erosion on Mediterranean vineyards. A review based on published data. *EGU General Assembly Conference Abstracts*, 17: 4034.

Shi Z, Ai L, Li X *et al*., 2013. Partial least-squares regression for linking land-cover patterns to soil erosion and sediment yield in watersheds. *Journal of Hydrology*, 498: 165–176.

Wei H, Fan W, Ding Z *et al*., 2017. Ecosystem services and ecological restoration in the northern Shaanxi Loess Plateau, China, in relation to climate fluctuation and investments in natural capital. *Sustainability*, 9(2): 199.

Wei Wei, Chen Liding, Fu Bojie *et al*., 2006. Soil and water loss affected by landuse under different rainfall patterns in the semi-arid loess hilly area. *Bulletin of Soil and Water Conservation*, 26(6): 19–23. (in Chinese)

Wu Linna, Yang Sheng Tian, Liu Xiaoyan *et al*., 2014. Response analysis of land use change to the degree of human activities in the Beiluo River basin since 1976. *Acta Geographica Sinica*, 69(1): 54–63. (in Chinese)

Zhang Wenbo, Fu Jinsheng, 2003. Rainfall erosivity estimation under different rainfall amount. *Resources Science*, 25(1): 35–41. (in Chinese)

Zhao W W, Fu B J, Chen L D, 2012. A comparison between soil loss evaluation index and the C-factor of RUSLE: A case study in the Loess Plateau of China. *Hydrology and Earth System Sciences*, 16(8): 2739–2748.

Zhao Wenwu, Fu Bojie, Guo Xudong, 2008. The methods and GIS techniques for calculating multi-scale soil loss evaluation index. *Progress in Geography*, 27(2): 47–52. (in Chinese)

Zhong Lina, 2015. Analysis of multi-scale effect of rainfall pattern and land use pattern on soil erosion: A case study in the hilly and gully area of the Loess Plateau. Beijing: Beijing Normal University. (in Chinese)

Zhong Lina, Zhao Wenwu, 2013. Detecting the dynamic changes of vegetation coverage in the Loess Plateau of China using NDVI data. *Science of Soil and Water Conservation*, 11(5): 57–62. (in Chinese)

Zhuang Jianqi, Ge Yonggang, 2012. Assessment of the soil loss associated with land use and precipitation change in the Xiaojiang River basin, Southwest China. *Resources and Environment in the Yangtze Basin*, 21(3): 288–295. (in Chinese)